Broadband Antenna Radiation Pattern Measurement From Backscattering Coefficient in a Reverberation Chamber

Francois Sarrazin, Ariston Reis, Lotfy Zeghoudi, Philippe Besnier, Elodie Richalot

Broadband Antenna Radiation Pattern Measurement From Backscattering Coefficient in a Reverberation Chamber

François Sarrazin[#1], Ariston Reis[#2], Lotfy Zeghoudi[#3], Philippe Besnier[*4], Elodie Richalot[#5]
[#]Univ Gustave Eiffel, CNRS, ESYCOM, F-77454 Marne-la-Vallée, France
[*]Univ Rennes, INSA Rennes, CNRS, IETR-UMR 6164, F-35000 Rennes, France
{[1]francois.sarrazin, [2]ariston.reis, [5]elodie.richalot-taisne}@univ-eiffel.fr, [4]philippe.besnier@insa-rennes.fr

***Abstract* — This paper deals with the contactless measurement of the radiation pattern of a log-periodic antenna within a reverberation chamber (RC). This method relies on backscattering measurement, i.e., avoiding to connect the antenna under test (AUT) to any analyzer, for two distinct AUT load conditions. The post-processing is based on a sinusoidal regression applied on the difference between the reflection coefficients measured for the two load conditions. A critical parameter to estimate is the frequency of the sinusoidal regression that depends here on the distance between the measurement antenna and the AUT. It is shown in this paper that the variation of the antenna phase center as a function of frequency has to be taken into account.**

***Keywords* — antenna, antenna measurement, backscattering measurement, contactless, phase center, reverberation chamber, radiation pattern.**

I. Introduction

Antenna characterization methods usually rely on a transmission-type setup between a measurement antenna and the antenna under test (AUT). This implies an invasive setup in which the AUT needs to be fed by a coaxial cable in order to measure its scattering coefficients S. This leads to undesired interactions between the AUT and its excitation cable. Although it may be negligible for large antennas, this effect becomes critical when dealing with electrically small antennas [1]. Indeed, due to the limited-size ground plane, the presence of the cable in the reactive zone of the AUT disturbs both its impedance and radiation characteristics [2]. To avoid this problem, some works focus on limiting the cables influence by adding ferrites for example [3], whereas another approach is to simply avoid the use of cables by performing backscattering measurement (non-invasive measurement).

Antenna scattering has been studied since 1950s [4]. The field backscattered by an antenna can be decomposed into two different modes: the structural mode, that is due to scattering of the antenna as any metallic object, and the radiation mode, that is due to the re-reflection by the AUT of the field received at its port. Many approaches in anechoic chambers have been proposed in order to distinguish between the two modes as only the radiation mode needs to be taken into account in order to retrieve antenna properties. They are based on load modulation, either by using transmission line of various lengths [5] or discrete load impedances [6].

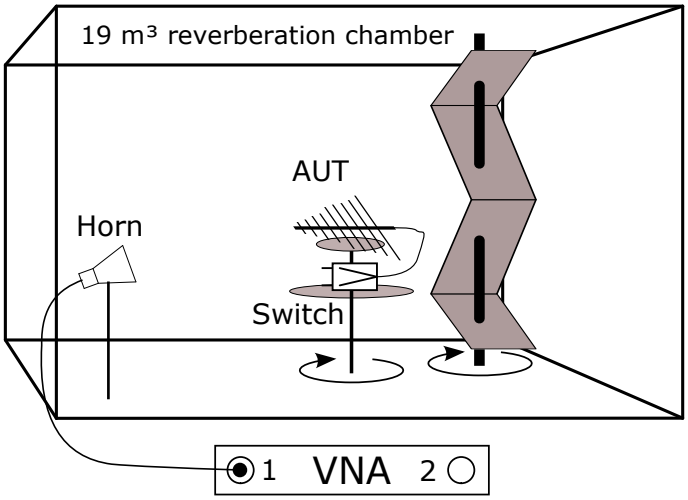

Fig. 1. Schematic view of the measurement setup. A horn antenna, connected to a VNA, is oriented towards the AUT (log-periodic antenna). The AUT is connected to a mechanical switch through a 60-cm cable and is rotated around the azimutal axis in order to measure its radiation pattern.

For 20 years, reverberation chambers (RCs) become popular for antenna characterization, especially in order to retrieve antenna radiation efficiency [7], [8], [9], thanks to the statistically isotropic and homogeneous field that occurs inside such chambers. However, it has been shown that RCs can also be used to retrieve line-of-sight parameters [10], [11]. In particular, based on an original radar cross-section (RCS) measurement method [12], a contactless method to retrieve the antenna gain pattern within RCs has been introduced in 2021 [13]. This method relies on a sinusoidal regression process applied on an S-parameter difference for two different AUT load conditions. The first step of the regression process requires the determination of the propagation distance between the measurement antenna and the AUT, which is usually assumed constant over the considered frequency range. In this paper, we show how the displacement of the AUT phase center as a function of frequency may induce significant variations on the estimated propagation distance.

II. Measurement Method

The considered measurement setup is presented in Fig. 1. It takes place in an RC with a mechanical stirrer whose position is denoted α. A measurement antenna is connected to a VNA and is oriented towards the AUT which rotates according to θ and which is terminated by a load impedance whose reflection coefficient is noted Γ_{L}. In this configuration, the reflection coefficient $S(f,\alpha,\theta,\Gamma_{\mathrm{L}})$ can be expressed as:

$$S(f,\alpha,\theta,\Gamma_{\mathrm{L}}) = S_{\mathrm{FS}}(f) + \left(1-|S_{\mathrm{FS}}(f)|^2\right)\eta \times [H(f,\alpha,\theta,\Gamma_{\mathrm{L}}) + h_{\mathrm{s}}(f,\alpha)] + C(f)\times\sqrt{\sigma(f,\theta,\Gamma_{\mathrm{L}})} \quad (1)$$

where $S_{\mathrm{FS}}(f)$ and η are respectively the free-space reflection coefficient and the radiation efficiency of the measurement antenna, $H(f,\alpha,\theta,\Gamma_{\mathrm{L}})$ is the RC transfer function associated to the diffuse field (its real and imaginary parts follow a Gaussian distribution), $h_{\mathrm{s}}(f,\alpha)$ is the transfer function describing the specular reflections. The term $C(f)\times\sqrt{\sigma(f,\theta,\Gamma_{\mathrm{L}})}$ describes the field backscattered by the AUT, $\sqrt{\sigma(f,\theta,\Gamma_{\mathrm{L}})}$ being the AUT backscattering coefficient, and $C(f)$ a complex amplitude that can be deduced from the Friis equation as:

$$C(f) = \frac{G(f)\lambda\left(1-|S_{\mathrm{FS}}(f)|^2\right)}{(4\pi)^{3/2}R^2}\exp\left(-\mathrm{j}2\pi f\frac{2R}{c}\right) \quad (2)$$

where $G(f)$ is the measurement antenna gain, c is the speed of light, λ is the wavelength and R is the propagation distance between the measurement antenna and the AUT. The AUT backscattering coefficient can be split into a structural $\sqrt{\sigma_{\mathrm{s}}(f,\theta)}$ and a radiation mode $\sqrt{\sigma_{\mathrm{r}}(f,\theta,\Gamma_{\mathrm{L}})}$ as follows:

$$\sqrt{\sigma(f,\theta,\Gamma_{\mathrm{L}})} = \sqrt{\sigma_{\mathrm{s}}(f,\theta)} + \sqrt{\sigma_{\mathrm{r}}(f,\theta,\Gamma_{\mathrm{L}})}. \quad (3)$$

It has to be noted that the structural mode does not depend on Γ_{L} whereas $\sqrt{\sigma_{\mathrm{r}}(f,\theta,\Gamma_{\mathrm{L}})}$ can be expressed as:

$$\sqrt{\sigma_{\mathrm{r}}(f,\theta,\Gamma_{\mathrm{L}})} = \sqrt{\sigma_{\mathrm{r}}^{\max}(f,\theta)}\times\Gamma_{\mathrm{L}}(f) \quad (4)$$

where $\sqrt{\sigma_{\mathrm{r}}^{\max}(f,\theta)}$ is the AUT backscattering coefficient due to the radiation mode for an ideal reflective load ($\Gamma_{\mathrm{L}}=1$). By computing the reflection coefficient difference for two load conditions Γ_{L1} and Γ_{L2}, it comes:

$$S(f,\alpha,\theta,\Gamma_{\mathrm{L1}}) - S(f,\alpha,\theta,\Gamma_{\mathrm{L2}}) = C(f)\times\sqrt{\sigma_{\mathrm{r}}^{\max}(f,\theta)}\times(\Gamma_{\mathrm{L1}}(f)-\Gamma_{\mathrm{L2}}(f)) + \left(1-|S_{\mathrm{FS}}(f)|^2\right)\eta\times[H(f,\alpha,\theta,\Gamma_{\mathrm{L1}}) - H(f,\alpha,\theta,\Gamma_{\mathrm{L2}})]. \quad (5)$$

This difference allows vanishing both $h_{\mathrm{s}}(f,\alpha)$ and $\sqrt{\sigma_{\mathrm{s}}(f,\theta)}$ as the specular reflections and the structural mode remain the same for both cases. The right-hand side of (5) is composed of two terms. The first one is proportional to the AUT radiation mode $\sqrt{\sigma_{\mathrm{r}}^{\max}(f,\theta)}$ and therefore to the AUT gain. The second term is proportional to the difference of two random variables whose real and imaginary parts are distributed according to a centered Gaussian probability density function with equal variance. By dividing the previous equation by $|C(f)|\times(\Gamma_{\mathrm{L1}}(f)-\Gamma_{\mathrm{L2}}(f))$, its real part can be re-written as:

$$\Re\left(\Delta_S(f,\theta,\Gamma_{\mathrm{L1}},\Gamma_{\mathrm{L2}})\right) = \sqrt{\sigma_{\mathrm{r}}^{\max}(f,\theta)}\times\cos\left(2\pi f\frac{2R}{c}\right) + n(f,\alpha,\theta) \quad (6)$$

where $n(f,\alpha,\theta)$ is the additive noise due to RC reflections and

$$\Delta_S(f,\theta,\Gamma_{\mathrm{L1}},\Gamma_{\mathrm{L2}}) = \frac{\langle S(f,\alpha,\theta,\Gamma_{\mathrm{L1}}) - S(f,\alpha,\theta,\Gamma_{\mathrm{L2}})\rangle_\alpha}{G(f)\lambda\left(1-|S_{\mathrm{FS}}(f)|^2\right)\times(\Gamma_{\mathrm{L1}}(f)-\Gamma_{\mathrm{L2}}(f))}. \quad (7)$$

where $\langle\cdot\rangle_\alpha$ is an ensemble average performed over the stirrer positions α which allows reducing the noise [14], [12]. We can notice that $\Re\left(\Delta_S(f,\theta,\Gamma_{\mathrm{L1}},\Gamma_{\mathrm{L2}})\right)$ behaves as a sine signal as a function of frequency with a $c/2R$ period. Therefore, the retrieval of $\sqrt{\sigma_{\mathrm{r}}^{\max}(f,\theta)}$ can be performed thanks to a sinusoidal regression (see [13] for details). Once $\sqrt{\sigma_{\mathrm{r}}^{\max}(f,\theta)}$ is known, the AUT gain $G_{\mathrm{AUT}}(f,\theta)$ can be computed as [15]:

$$G_{\mathrm{AUT}}(f,\theta) = \frac{\sqrt{4\pi}}{\lambda}\times\sqrt{|\sigma_{\mathrm{r}}^{\max}(f,\theta)|}. \quad (8)$$

III. Results

A. Measurement setup

The experiment is performed in a 19 m^3 RC at the ESYCOM laboratory. It is equipped with a rotating Z-fold mode stirrer and 72 equally-spaced positions have been considered to perform the mechanical stirring. The AUT is a log-periodic antenna Schwarzbeck VUSLP 9111. It is positioned on top of a rotating mast ($-32^\circ < \theta < 32^\circ$, $\theta = 0^\circ$ being the boresight direction) and is connected to a remotely-controlled mechanical switch through a 60-cm coaxial cable. Two different terminations are connected to the switch: an open circuit (OC) and a 50 Ω load. A horn antenna, oriented towards the AUT, is connected to a VNA in order to measure its reflection coefficient in the 1.5 GHz to 4 GHz (25001 frequency points).

The difference between the reflection coefficients for the two load impedances is presented in Fig. 2 as a function of frequency for $\theta = 0^\circ$ (boresight direction). We can observe the expected sinusoidal behavior in addition to which an additive Gaussian noise is present due to RC reflections. The decrease of the signal amplitude versus frequency is explained by the decreasing AUT gain in this frequency range. The post-process is composed of two steps: 1) Evaluation of the frequency period, related to the distance R, and 2) Application of a sinusoidal regression to evaluate the amplitude, and therefore the AUT gain.

B. Distance evaluation

The first step of the measurement post-process consists in evaluating the period of the observed sine wave. A Fourier transform is therefore performed in three different 1 GHz-wide

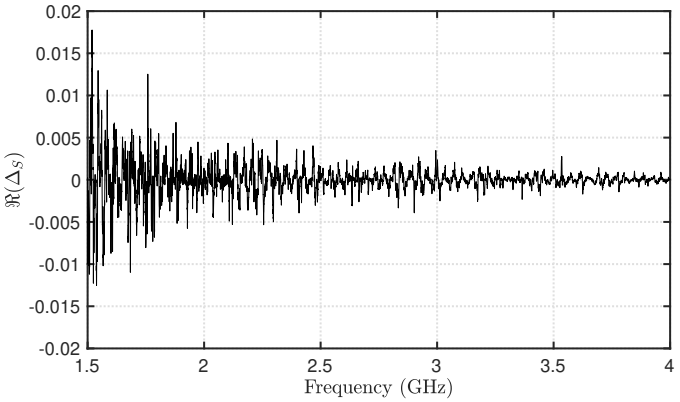

Fig. 2. Real part of Δ_S as a function of frequency for $\theta = 0°$.

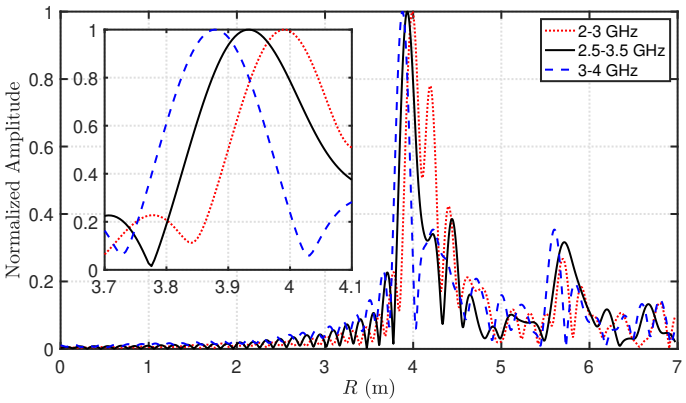

Fig. 3. Fourier Transform of $\Re(\Delta_S)$ expressed as a function of the distance R between the two antenna ports for three different frequency bandwidths for $\theta = 0°$.

frequency windows. Results are presented in Fig. 3 for $\theta = 0°$ and the x-axis is expressed in terms of a distance R between the two antenna ports (assuming a velocity equal to c). Firstly, we can notice that the evaluated distance R is equal to about 3.9 m. The physical distance between the two antenna apertures is about 2.2 m but the guided path between the antenna apertures and the antenna ports need to be added, explaining this difference. Secondly, in previous works [12], [13], R was supposed constant over the frequency bandwidth. However, we can see here that the estimated R tends to decrease when the frequency increases.

In order to deeper analyze the R variation as a function of frequency, we compute the distance corresponding to the maximum of the Fourier transform for a 1 GHz-wide sliding window in the entire frequency range. Results are presented in Fig. 4 for three θ values. We can see that the distance slowly decreases as a function of frequency. This can be explained by the displacement of the AUT phase center. When the frequency increases, the antenna phase center becomes closer to the antenna port, leading to smaller guided propagation (higher radiated propagation), and therefore a smaller equivalent distance. Also, the estimated R slightly varies according to θ with an average difference of 1.7 cm

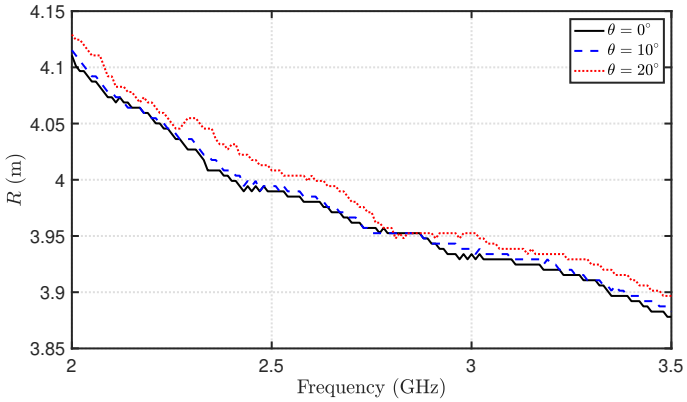

Fig. 4. Estimated propagation distance R as a function of frequency for $\theta = \{0°, 10°, 20°\}$.

between $\theta = 0°$ and $\theta = 20°$ (maximum difference of 3.6 cm). This can be attributed to the AUT rotation axis being not exactly positioned at the AUT phase center.

C. Radiation Pattern Estimation

Once R is known, the sinusoidal regression can be performed to evaluate the sine amplitude. It is noted that R is estimated for each θ in order to take into account the small variations seen in Fig. 4. Fig. 5 presents the antenna radiation pattern obtained using the RC contactless method at two different frequencies: 3 GHz and 3.5 GHz, both using a 1 GHz-wide frequency bandwidth. Results are compared to classical transmission-type anechoic chamber (AC) measurement that have been performed at the same distance between the two antennas and in which the AUT rotates around the same axis. The maximum gain is normalized by the gain values obtained from the antenna datasheet for both measurements. We can see a good agreement between the two measurements at both frequencies with a maximum difference minor than 1.5 dB.

IV. Conclusion

In this paper, the contactless antenna radiation pattern measurement method within RC introduced in [13] has been applied to characterize a wideband log-periodic antenna in the 1.5 GHz to 4 GHz frequency range. This method requires the use of a sinusoidal regression whose first step is to evaluate the period of the signal, related here to the equivalent distance between the measurement antenna and the AUT. We highlighted in this paper that, when dealing with wideband antennas, this equivalent distance may vary as a function of frequency due to the modification of the antenna phase center. By properly taking into account this variation, results obtained through the RC contactless measurement setup are in good agreement with conventional transmission-type AC measurement.

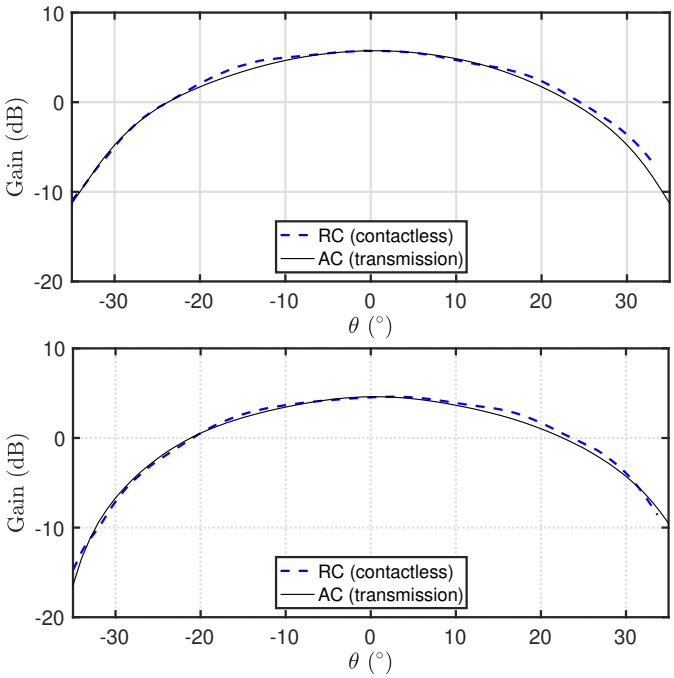

Fig. 5. AUT radiation pattern estimated using the contactless RC method (1 GHz frequency bandwidth) and compared with conventional transmission-type anechoic chamber measurement: 3 GHz (top) and 3.5 GHz (bottom).

REFERENCES

[1] L. Huitema, C. Delaveaud, and R. D'Errico, "Impedance and radiation measurement methodology for ultra miniature antennas," *IEEE Transactions on Antennas and Propagation*, vol. 62, no. 7, pp. 3463–3473, 2014.

[2] J. DeMarinis, "The antenna cable as a source of error in emi measurements," in *IEEE 1988 International Symposium on Electromagnetic Compatibility*, 1988, pp. 9–14.

[3] C. Icheln, J. Ollikainen, and P. Vainikainen, "Reducing the influence of feed cables on small antenna measurements," *Electronics Letters*, vol. 35, pp. 1212–1214, 1999.

[4] D. D. King, "The measurement and interpretation of antenna scattering," *Proceedings of the IRE*, vol. 37, pp. 770–777, 1949.

[5] J. Appel-Hansen, "Accurate determination of gain and radiation patterns by radar cross-section measurements," *IEEE Transactions on Antennas and Propagation*, vol. 27, no. 5, pp. 640–646, 1979.

[6] W. Wiesbeck and E. Heidrich, "Wide-band multiport antenna characterization by polarimetric RCS measurements," *IEEE Transactions on Antennas and Propagation*, vol. 46, no. 3, pp. 341–350, 1998.

[7] C. L. Holloway, H. A. Shah, R. J. Pirkl, W. F. Young, D. A. Hill, and J. Ladbury, "Reverberation chamber techniques for determining the radiation and total efficiency of antennas," *IEEE Transactions on Antennas and Propagation*, vol. 60, no. 4, pp. 1758–1770, 2012.

[8] W. Krouka, F. Sarrazin, J. d. Rosny, A. Labdouni, and E. Richalot, "Antenna radiation efficiency estimation from backscattering measurement performed within reverberation chambers," *IEEE Transactions on Electromagnetic Compatibility*, pp. 1–8, 2021.

[9] W. Krouka, F. Sarrazin, J. Sol, P. Besnier, and E. Richalot, "Biased estimation of antenna radiation efficiency within reverberation chambers due to unstirred field: Role of antenna stirring," *IEEE Transactions on Antennas and Propagation*, pp. 1–1, 2022.

[10] M. García-Fernández, D. Carsenat, and C. Decroze, "Antenna gain and radiation pattern measurements in reverberation chamber using doppler effect," *IEEE Transactions on Antennas and Propagation*, vol. 62, no. 10, pp. 5389–5394, 2014.

[11] A. Soltane, G. Andrieu, E. Perrin, C. Decroze, and A. Reineix, "Antenna radiation pattern measurement in a reverberating enclosure using the time-gating technique," *IEEE Antennas and Wireless Propagation Letters*, vol. 19, no. 1, pp. 183–187, 2020.

[12] A. Reis, F. Sarrazin, E. Richalot, S. Méric, J. Sol, P. Pouliguen, and P. Besnier, "Radar cross section pattern measurements in a mode-stirred reverberation chamber: Theory and experiments," *IEEE Transactions on Antennas and Propagation*, vol. 69, no. 9, pp. 5942–5952, 2021.

[13] A. Reis, F. Sarrazin, P. Besnier, P. Pouliguen, and E. Richalot, "Contactless antenna gain pattern estimation from backscattering coefficient measurement performed within a reverberation chamber," *IEEE Transactions on Antennas and Propagation*, vol. 70, no. 3, pp. 2318–2321, 2022.

[14] A. Reis, F. Sarrazin, E. Richalot, and P. Pouliguen, "Mode-stirring impact in radar cross section evaluation in reverberation chamber," in *2018 International Symposium on Electromagnetic Compatibility (EMC EUROPE)*, 2018, pp. 875–878.

[15] E. F. Knott, *Radar Cross Section*. Institution of Engineering and Technology, 2004. [Online]. Available: https://digital-library.theiet.org/content/books/ra/sbra026e